Structural distortions favoring magnetization enhancement near the $SrRuO_3/Sr_2RuO_4$ interface

A. O. Mufazalova,[1] A. S. Belozerov,[1,2] and S. V. Streltsov[1,2]
[1]*Ural Federal University, 620002 Yekaterinburg, Russia*
[2]*M. N. Miheev Institute of Metal Physics, Russian Academy of Sciences, 620137 Yekaterinburg, Russia*

(Received 1 August 2018; revised manuscript received 24 September 2018; published 24 October 2018)

Using *ab initio* methods we successfully reproduce an unusual enhancement of magnetization experimentally observed in ferromagnetic $SrRuO_3$ thin films deposited on the spin-triplet superconductor Sr_2RuO_4. We found that this enhancement is due to additional distortions of Sr_2RuO_4 induced by the film. These distortions—rotation of the RuO_6 octahedra—lead to a gradual reconstruction of electronic structure of the substrate, such that the Fermi level turns out to be exactly at the peak of the local density of states, corresponding to the Ru ions close to the interface. This results in the magnetic instability. The distortions propagate deep into the substrate and favor the formation of magnetic moments on the Ru ions in Sr_2RuO_4 near the interface. Our estimates show that these distortions may penetrate into Sr_2RuO_4 substrate up to 40 nm in depth, which agrees with experimental observations.

DOI: 10.1103/PhysRevB.98.134441

I. INTRODUCTION

The ferromagnet/superconductor heterostructures are of special interest due to their potential applications in superconducting spintronics. Although the spin-singlet superconductors can be used for the induction of spin-polarized supercurrent in ferromagnetic (FM) metals, the usage of spin-triplet superconductors has certain advantages. Recently, the penetration of spin-triplet superconductivity of Sr_2RuO_4 into an FM metal $SrRuO_3$ has been found in $Au/SrRuO_3/Sr_2RuO_4$ junctions [1]. However, layered structures based on the combination of $SrRuO_3$ and Sr_2RuO_4 are also very interesting from the point of view of magnetic properties.

While Sr_2RuO_4 is paramagnetic above 1.5 K (below it is superconducting), the epitaxial thin film of $SrRuO_3$ grown on the (001) surface of Sr_2RuO_4 was shown to induce magnetization $\sim 3\mu_B$/Ru [2,3]. This even exceeds the upper limit of $2\mu_B$ for the spin moment of the Ru^{4+} ion in the low-spin state [electronic configuration $(t_{2g}^{\uparrow})^3(t_{2g}^{\downarrow})^1$]. Thus, one may even expect stabilization of the high-spin state $[(t_{2g}^{\uparrow})^3(e_g^{\uparrow})^1]$ in this system, but this is rather unlikely due to very large $t_{2g} - e_g$ crystal-field splitting [4]. The Curie temperature of the film $T_C \approx 160$ K stays nearly the same as in bulk $SrRuO_3$, although the film is under 1.7% in-plane compressive strain [2,3,5].

Considering $SrRuO_3$ films on different perovskite substrates with different substrate-induced strains, Lee *et al.* [5] demonstrated that the anomalous enhancement of magnetization occurs only with the Sr_2RuO_4 substrate: in this case, the magnetization is nearly twice as large as for other substrates. Thus, the enhanced magnetization is not due to distortions induced in the film by the strains. Moreover, increase of the magnetization occurs not in the film, but in the substrate [5]. Why the film is able to change magnetic properties of the substrate, how important the carrier induction to the substrate is, and what is in principle the microscopic mechanism lying behind this effect remain obscure.

In the present paper, we shed some light on this phenomenon using first-principles calculations. The density functional theory is able to reproduce experimentally observed enhancement of the magnetic moment in Sr_2RuO_4 layers in vicinity of the interface. This is due to distortions of Sr_2RuO_4 induced by the $SrRuO_3$ film. Moreover, these distortions were found to easily propagate into the substrate. This explains why this effect is not restricted by interface only, but was observed experimentally in the Sr_2RuO_4 substrate at the depths of order tenth nanometers.

II. COMPUTATIONAL DETAILS

To simulate a thin film of $SrRuO_3$ grown on *ab* surface of Sr_2RuO_4, we built a superlattice structure consisting of two layers of $SrRuO_3$ deposited on SrO-terminated five layers of Sr_2RuO_4 as depicted in Fig. 1. Each layer in the considered supercell of 90 atoms is presented by two ruthenium atoms in the oxygen octahedra. To eliminate the interaction between periodic images, we also included a vacuum layer of 15 Å and checked the convergence with respect to its thickness.

Our calculations were carried out using the pseudopotential plane-wave method implemented in the QUANTUM-ESPRESSO (QE) package [6]. The Vanderbilt ultrasoft pseudopotentials from the QE library were used. The exchange-correlation potential was considered in the Perdew-Burke-Ernzerhof form of generalized gradient approximation (GGA). The convergence threshold of 10^{-6} Ry/atom was used for total energy. The kinetic energy cutoff for wave functions was set to 40 Ry. Magnetic moments were calculated using projection of plane waves onto orthogonalized atomic wave functions. We used the experimental lattice constants at 15 K for Sr_2RuO_4 [7], at 1.5 K for orthorhombic $SrRuO_3$ [8], and at 823 K for tetragonal $SrRuO_3$ [9]. To deposit the layers of $SrRuO_3$ on Sr_2RuO_4, the former were considered in the tetragonal structure and in-plane compressed to match the lattice parameter of the substrate as in epitaxially grown films. This induces strains, which were recently found to be very important for Sr_2RuO_4 since they change the fermiology and may even result to the Lifshitz transition [11–13].

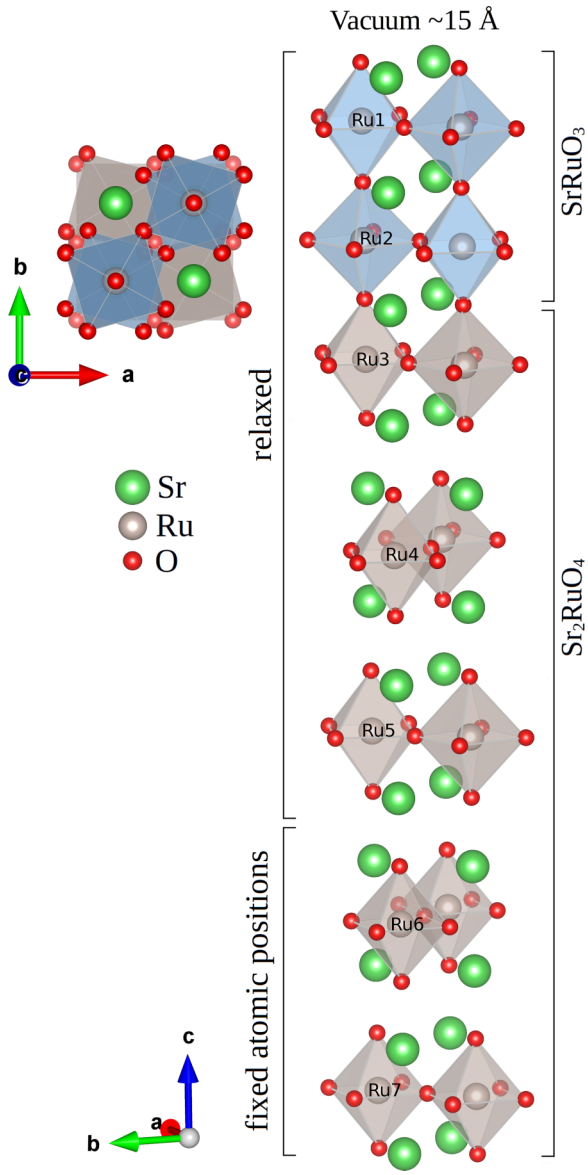

FIG. 1. Structure consisting of two layers of $SrRuO_3$ deposited on five layers of Sr_2RuO_4 in top view (left) and side view (right). In our calculations, a vacuum layer of 15 Å was introduced to separate the periodic images of the presented structure. The atomic positions were obtained by the structural relaxation within GGA. The figure was prepared with the VESTA program [10].

Subsequently, the structural relaxation was performed for the atomic positions of the film and three layers of the substrate near the interface to take into account strain effects. The atoms were relaxed until the force on each atom was less than 25 meV/Å. Integration in reciprocal space was performed using $14 \times 14 \times 1$ Monkhorst-Pack **k**-point grid for the considered supercell of 90 atoms.

III. RESULTS AND DISCUSSION

A. Bulk $SrRuO_3$, Sr_2RuO_4, and their monolayers

We start with the GGA calculations of bulk $SrRuO_3$ and Sr_2RuO_4. Main results are summarized in Table I. One may see that calculated magnetic moments on the Ru ions are close to what has been previously obtained. In particular, in bulk $SrRuO_3$ we have $\sim 1.3\ \mu_B$ for an orthorhombic structure and $\sim 1.2\ \mu_B$ for a tetragonal one, while in previous studies it was found to be $\sim 1.2\ \mu_B$ [14,15]. In bulk Sr_2RuO_4, we obtained $0.38\ \mu_B$, which is close to $0.25\ \mu_B$ obtained in previous GGA calculations [16].

TABLE I. Local magnetic moments obtained in GGA calculations for $SrRuO_3$, Sr_2RuO_4, and relaxed $SrRuO_3/Sr_2RuO_4$ slab presented in Fig. 1.

Compound	Atom	Moment (μ_B)
$SrRuO_3$ (bulk, orthorhombic)	Ru	1.28
$SrRuO_3$ (bulk, tetragonal)	Ru	1.21
$SrRuO_3$ (monolayer, tetragonal)	Ru	1.31
Sr_2RuO_4 (bulk)	Ru	0.38
Sr_2RuO_4 (monolayer)	Ru	0.49
$SrRuO_3/Sr_2RuO_4$ (relaxed)	Ru1 ($SrRuO_3$)	1.29
	Ru2 ($SrRuO_3$)	1.37
	Ru3 (Sr_2RuO_4)	1.30
	Ru4 (Sr_2RuO_4)	1.28
	Ru5 (Sr_2RuO_4)	1.28
	Ru6 (Sr_2RuO_4)	0.42
	Ru7 (Sr_2RuO_4)	0.53

Next we studied isolated monolayers (MLs) containing RuO_6 octahedra in the ab plane with termination on SrO surface. These MLs were separated by a vacuum layer of 15 Å along the c axis. In the case of $SrRuO_3$, where the oxygen octahedra are rotated forming Ru-O-Ru angle of 168.4°, the magnetic moments on the Ru ions were found to be 1.31 μ_B, i.e., nearly the same as in the bulk. This agrees with results of the previous study [17]. Thus, we see that a low dimensionality by itself has a minor effect on the magnetic properties of $SrRuO_3$. For an ML of Sr_2RuO_4, where the octahedra are not rotated, the obtained magnetic moment of $0.49\ \mu_B$ is also rather similar to its bulk counterpart.

B. Electronic structure of nonmagnetic $SrRuO_3/Sr_2RuO_4$ slab

As a second step, $SrRuO_3/Sr_2RuO_4$ slab was studied (details of the slab construction are described in Sec. II). We found that FM $SrRuO_3$ induces dramatic changes in both electronic and magnetic properties of Sr_2RuO_4, but we start with the nonmagnetic GGA calculations.

Figure 2 shows that in the nonmagnetic GGA calculations, the partial density of states (DOS) corresponding to the Ru ions belonging to $SrRuO_3$ film (Ru1 and Ru2) are nearly the same as in bulk $SrRuO_3$. The partial density of states corresponding to Ru2, i.e., Ru ion exactly at the interface (but on the $SrRuO_3$ side), is very similar to the DOS of bulk $SrRuO_3$. The DOS of Ru1 in contrast has an additional peak at ≈ -1.2 eV. This is due to the fact that this Ru is on the border of the film and vacuum. Therefore, Ru1 is in some sense halfway to layered Sr_2RuO_4, where different RuO_2 layers are separated from each other by two SrO layers. A similar peak at ≈ -1.2 eV is clearly seen in bulk Sr_2RuO_4.

The local DOS of the first three Ru ions in the substrate (Ru3, Ru4, Ru5; these are ions allowed to relax) have features of both $SrRuO_3$ and Sr_2RuO_4. There is a pronounced peak

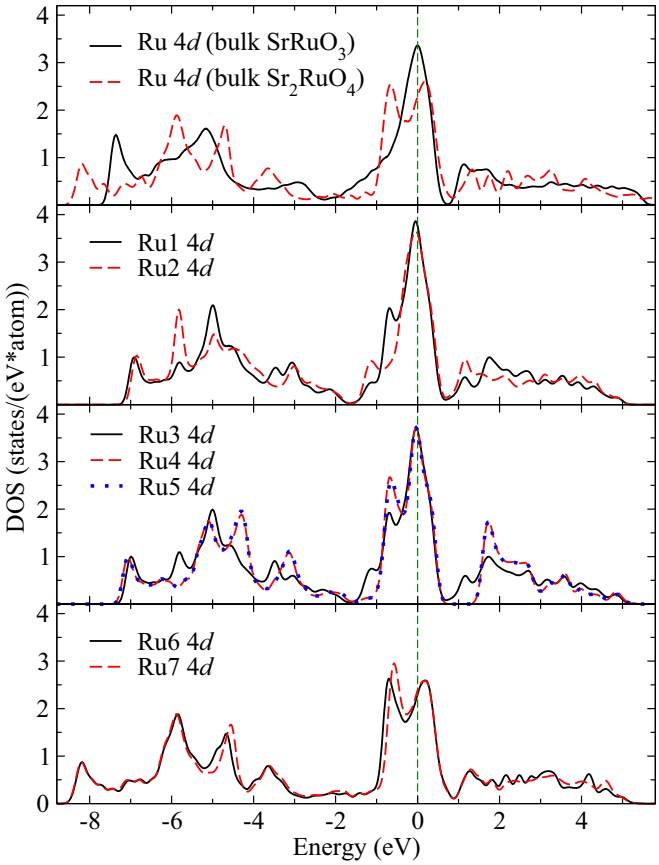

FIG. 2. Density of Ru 4*d* states for bulk $SrRuO_3$ and Sr_2RuO_4 (top panel), as well as for the structure with two layers of $SrRuO_3$ deposited on five layers of Sr_2RuO_4 as obtained by nonmagnetic GGA calculations. The numeration of ruthenium atoms is depicted in Fig. 1. The Fermi level is at zero energy.

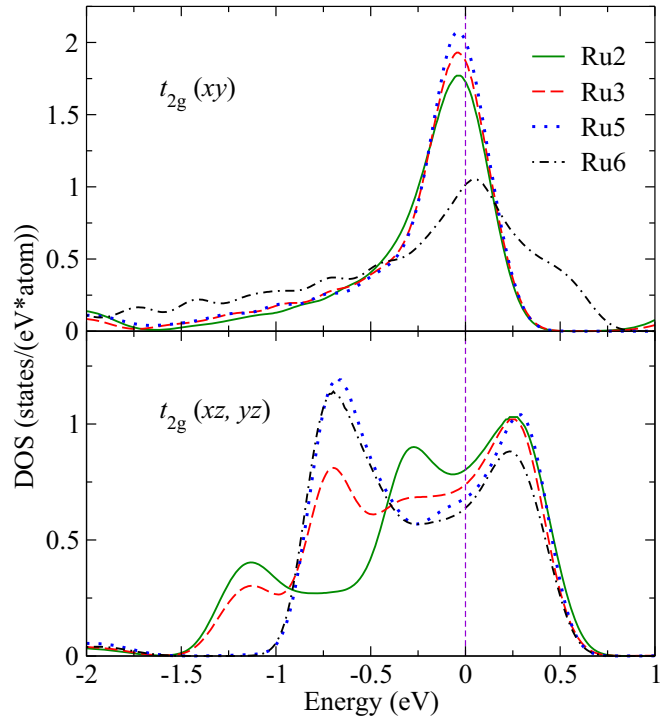

FIG. 3. Orbital-projected density of Ru t_{2g} states for the structure with two layers of $SrRuO_3$ deposited on five layers of Sr_2RuO_4 as obtained by nonmagnetic GGA calculations. The numeration of ruthenium atoms is depicted in Fig. 1. The Fermi level is at zero energy.

exactly at the Fermi level and smaller peak at ≈ -1.2 eV, which is a precursor of the low-energy peak in the t_{2g} DOS of bulk Sr_2RuO_4. The fact that the Fermi energy turns out to be at maximum of the nonmagnetic DOS results in magnetic instability, which favors formation of relatively large (with respect to bulk Sr_2RuO_4) magnetic moments and FM order as in bulk $SrRuO_3$ or $BaRuO_3$ [14,18]. The deepest Ru6 and Ru7 ions have exactly the same local DOS as bulk Sr_2RuO_4. Their positions were fixed in the calculations to simulate thick Sr_2RuO_4 substrate.

The Ru 4*d* states near the Fermi level are mainly of the t_{2g} symmetry, while the e_g states lie higher in energy due to the octahedral crystal field splitting. In Fig. 3, we show the orbitally resolved t_{2g} DOS obtained as a projection onto orthogonalized atomic wave functions in a local coordinate system with axes pointed to oxygen atoms. For all relaxed Ru ions (Ru1–Ru5), the density of xy states has a pronounced peak almost at the Fermi level, which is similar to that of bulk $SrRuO_3$. At the same time, Ru6 and Ru7 with fixed atomic positions have nearly the same Ru-xy DOS as bulk Sr_2RuO_4. In this case, the xy bandwidth is significantly larger than that of the relaxed ions, since the oxygen octahedra are not rotated (Ru-O-Ru angle is 180°) resulting in a larger hybridization with corresponding orbitals of neighbor atoms.

The layered structure of bulk Sr_2RuO_4 leads to a nearly one-dimensional character of the xz and yz bands, which is clearly seen in Fig. 3 for Ru5 and Ru6 located far from the interface. For Ru3 located in Sr_2RuO_4 substrate near the interface, the density of the xz and yz states partly loses its one-dimensional shape, which is completely lost for Ru2 in the film, where the RuO_2 layers separated only by one layer of SrO.

C. Magnetic properties of $SrRuO_3/Sr_2RuO_4$ slab

The DOS plot in magnetic GGA calculation is shown in Fig. 4. The reconstruction of the electronic structure inevitably affects the magnetic properties of the slab. The list of the magnetic moments obtained for different Ru ions is given in Table I. One may see that in the film (Ru1 and Ru2) they are nearly the same as in bulk $SrRuO_3$. Moreover, magnetic moments of the first three layers of the substrate (Ru3, Ru4, Ru5) are also of order of 1.2 μ_B. While lowest two Ru ions (Ru6 and Ru7) have moments similar to bulk Sr_2RuO_4.

The origin of this difference is in the way how our slab was constructed (see also Sec. II). To simulate a massive substrate, we had to fix positions of Ru ions in two lowest layers as in bulk Sr_2RuO_4, while all other Ru ions (including those of the film) were allowed to relax. These fixed Ru6 and Ru7 have both the electronic structure and magnetic moments very similar to bulk Sr_2RuO_4. Modification of the crystal structure of other layers results in enhancement of the magnetic moments of Ru ions in these layers. In Table II, we

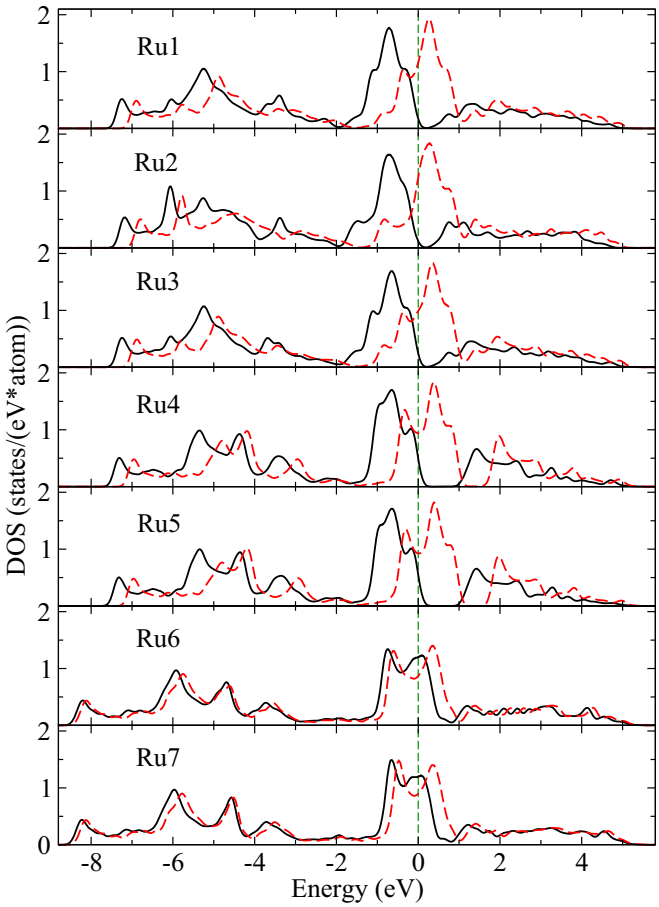

FIG. 4. Results of magnetic calculations. Density of Ru 4*d* states for the structure with two layers of $SrRuO_3$ deposited on five layers of Sr_2RuO_4. Different line types are used for different spin projections. The numeration of ruthenium atoms is depicted in Fig. 1. The Fermi level is at zero energy.

present results of additional calculations, where not only two lowest, but all substrate layers were not allowed to relax. One may see that in this situation magnetic moment increases only in the first Sr_2RuO_4 layer, i.e., just at the interface.

Thus, we see that structural distortions are very important for formation of magnetic moments in $SrRuO_3/Sr_2RuO_4$. However, there can be an additional mechanism—carrier redistribution, which may stabilize large magnetic moments, as it occurs, e.g., in Sr_2RuO_4 doped by Co [19]. To eliminate doping effects we constructed the bulk Sr_2RuO_4 structure, distorted exactly as Sr_2RuO_4 substrate near the interface. We choose the structure corresponding to the Ru4 layer of our slab (but equally well one may take the Ru3 or Ru5 layers). Magnetic moments on Ru ions in this model bulk Sr_2RuO_4 were found to be 1.26 μ_B, very close to 1.28 μ_B obtained for Ru4 in the $SrRuO_3/Sr_2RuO_4$ slab.

TABLE II. Local magnetic moments obtained in GGA calculations for unrelaxed $SrRuO_3/Sr_2RuO_4$ slab.

Compound	Atom	Moment (μ_B)
$SrRuO_3/Sr_2RuO_4$ (unrelaxed)	Ru1 ($SrRuO_3$)	1.24
	Ru2 ($SrRuO_3$)	1.26
	Ru3 (Sr_2RuO_4)	0.78
	Ru4 (Sr_2RuO_4)	0.40
	Ru5 (Sr_2RuO_4)	0.38
	Ru6 (Sr_2RuO_4)	0.38
	Ru7 (Sr_2RuO_4)	0.48

Therefore, our results demonstrate that these are not a doping or a charge redistribution, but the modification of the *substrate's* crystal structure, which is responsible for the increase of magnetic moments in $SrRuO_3/Sr_2RuO_4$. This structural reconstruction is possible because of the layered structure of Sr_2RuO_4, where SrO block layers frustrate structural coherence along the *c* axis. Due to computation limitations, we were able to calculate only the seven-layer $SrRuO_3/Sr_2RuO_4$ slab, but already this calculation shows that crystal structure of all layers in the substrate, which were allowed to relax, strongly changes. Thus, calculations suggest that structural reconstructions and increase of magnetic moment in real $SrRuO_3/Sr_2RuO_4$ may spread on many layers down to the substrate. This agrees with experimental finding of magnetization enhancement up to 20-nm depth of Sr_2RuO_4 [5].

However, only increase of the magnetic moments in the first 10–20 layers nearby the interface is not enough to explain growth of the magnetization observed experimentally. There must be not only larger magnetic moments in Sr_2RuO_4 due to proximity to $SrRuO_3$, but these larger moments in Sr_2RuO_4 also must order ferromagnetically. To check that magnetic moments tend to order in this way both along the *c* direction and in the *ab* plane, we calculated total energies of several additional configurations. First, the total energy of ferromagnetically coupled $SrRuO_3$ and Sr_2RuO_4 is on 4.7 meV/atom lower than the antiferromagnetically one (spins in the *ab* plane were ordered ferromagnetically). Second, the total energy of the slab with antiferromagnetic order of the Ru3 moments, i.e., exactly at the interface, is on 5.3 meV/atom higher than the one with FM order. This shows that both interlayer and intralayer exchange interactions are FM. We intentionally did not calculate the exchange interaction parameters (J) for the Heisenberg model from these values, since they would be overestimated: we optimized the crystal structure using FM order and thus there would be additional contribution to the total energy from the lattice.

D. Structural modifications in $SrRuO_3/Sr_2RuO_4$ slab

In this subsection, we discuss results of structural optimization of $SrRuO_3/Sr_2RuO_4$ slab in the GGA calculations. There is a misfit in lattice parameters between $SrRuO_3$ and Sr_2RuO_4, which results in a strain affecting crystal structure of the film and inducing compression in the *ab* plane and elongation along the *c* axis. The elongation of our film is about 7.2% and it was also observed in experiment. Three Ru layers of the substrate adjacent to the interface were also found to be stretched by 3.5%, 4.9%, and 4.8%.

Compression in the *ab* plane severely changes the rotation Ru-O-Ru angle from $\theta = 161.9^\circ$ in bulk $SrRuO_3$ to 148.0° in $SrRuO_3$ deposed on Sr_2RuO_4. Bulk Sr_2RuO_4 is tetragonal and therefore there should be no rotation of the RuO_6 deep in the substrate, but near the interface they may easily develop. Our calculations reveal that the rotation angle in the first layer

of Sr_2RuO_4 (i.e., at the interface; Ru3) is in fact about the same as in the film: 149.3°, i.e., it changes only on $\delta\theta = 1.3°$. This is not surprising, since the interface was designed via a direct sharing of oxygen ions between $SrRuO_3$ and Sr_2RuO_4 layers without intervening SrO layer. However, the distortion strength in the next Ru layer is not much smaller: the rotation angle is $\theta = 150.5°$ (Ru4 layer in Fig. 1), i.e., the layer-by-layer change is $\delta\theta = 1.2°$. In the next Ru layer, the rotation angle is $\theta = 151.0°$ (Ru5 layer in Fig. 1), i.e., the layer-by-layer change is $\delta\theta = 0.5°$.

Extrapolating these data, one might expect that the strain-induced distortions of the substrate penetrate over ∼60 layers or ∼40 nanometers in depth. However, at low distortions, the magnetic moments may be weak or even absent. Thus, our results are generally in agreement with the experimental estimate of over 20-nm penetration of magnetic moment induction into the Sr_2RuO_4 substrate [5].

Finally, we would like to mention that similar effects of substantial structural modifications were observed in $Sr_2RuO_4/Sr_3Ru_2O_7$ heterostructures [20,21]. Moreover, in the present paper, we assumed that there is a sharp transition from $SrRuO_3$ to Sr_2RuO_4 and no other Ruddlesden-Popper $Sr_{n+1}Ru_nO_{3n+1}$ ruthenates are formed at the interface. It would be very interesting to study this possibility theoretically.

IV. CONCLUSION

To sum up, in the present paper we demonstrate that there is a severe reconstruction of the substrate crystal structure in slab of $SrRuO_3$ film on the Sr_2RuO_4 substrate, which results in modification of the electronic structure in the vicinity of the interface, which in turn affects magnetic properties. These distortions are induced by the strains due to a mismatch in lattice parameters between the film and the substrate. They propagate through the lattice and, according to a rather crude estimation based on the results of present GGA calculations, may exceed ∼40 nanometers in depth. This is the reconstruction of the crystal structure and not injection of the electrons from the FM metallic film to the substrate, which results in enhanced magnetization of $SrRuO_3/Sr_2RuO_4$ observed experimentally. One may argue that the layered structure of the substrate frustrates a structural coherence along the c axis and favors long-range reconstruction of the crystal structure and enhancement of the magnetization in $SrRuO_3/Sr_2RuO_4$.

ACKNOWLEDGMENTS

We thank Y. Maeno for motivation and D. Khomskii for useful comments. Present work was supported by the project of the Ural branch of RAS 18-10-2-37, by the FASO through research programs "Electron" AAAA-A18-118020190098-5 and "Spin" AAAA-A18-118020290104-2, by the Russian Ministry of Science and High Education via Contract No. 02.A03.21.0006 and by the Russian Foundation for Basic Research (RFBR) via Grant No. RFBR 16-02-00451 and the Russian president council on science through program MD-916.2017.2.

[1] M. S. Anwar, S. R. Lee, R. Ishiguro, Y. Sugimoto, Y. Tano, S. J. Kang, Y. J. Shin, S. Yonezawa, D. Manske, H. Takayanagi, T. W. Noh, and Y. Maeno, Nat. Commun. **7**, 13220 (2016).

[2] M. S. Anwar, Y. J. Shin, S. R. Lee, S. J. Kang, Y. Sugimoto, S. Yonezawa, T. W. Noh, and Y. Maeno, Appl. Phys. Expr. **8**, 015502 (2015).

[3] Y. Sugimoto, M. S. Anwar, S. R. Lee, Y. J. Shin, S. Yonezawa, T. W. Noh, and Y. Maeno, Phys. Proc. **75**, 413 (2015).

[4] S. V. Streltsov and D. I. Khomskii, Phys. Usp. **60**, 1121 (2017).

[5] S. R. Lee, M. S. Anwar, Y. J. Shin, M.-C. Lee, Y. Sugimoto, M. Kunieda, S. Yonezawa, Y. Maeno, and T. W. Noh, arXiv:1609.03010.

[6] P. Giannozzi, S. Baroni, N. Bonini, M. Calandra, R. Car, C. Cavazzoni, D. Ceresoli, G. L. Chiarotti, M. Cococcioni, I. Dabo *et al.*, J. Phys: Condens. Matter **21**, 395502 (2009); **29**, 465901 (2017).

[7] O. Chmaissem, J. D. Jorgensen, H. Shaked, S. Ikeda, and Y. Maeno, Phys. Rev. B **57**, 5067 (1998).

[8] S. N. Bushmeleva, V. Yu. Pomjakushin, E. V. Pomjakushina, D. V. Sheptyakov, and A. M. Balagurov, J. Magn. Magn. Mater. **305**, 491 (2006).

[9] B. J. Kennedy and B. A. Hunter, Phys. Rev. B **58**, 653 (1998).

[10] K. Momma and F. Izumi, J. Appl. Crystallogr. **44**, 1272 (2011).

[11] Y.-T. Hsu, W. Cho, A. F. Rebola, B. Burganov, C. Adamo, K. M. Shen, D. G. Schlom, C. J. Fennie, and E.-A. Kim, Phys. Rev. B **94**, 045118 (2016).

[12] B. Burganov, C. Adamo, A. Mulder, M. Uchida, P. D. C. King, J. W. Harter, D. E. Shai, A. S. Gibbs, A. P. Mackenzie, R. Uecker, M. Bruetzam, M. R. Beasley, C. J. Fennie, D. G. Schlom, and K. M. Shen, Phys. Rev. Lett. **116**, 197003 (2016).

[13] A. Steppke, L. Zhao, M. E. Barber, T. Scaffidi, F. Jerzembeck, H. Rosner, A. S. Gibbs, Y. Maeno, S. H. Simon, A. P. Mackenzie, and C. W. Hicks, Science **355**, 148 (2017).

[14] I. I. Mazin and D. J. Singh, Phys. Rev. B **56**, 2556 (1997).

[15] C. Etz, I. V. Maznichenko, D. Böttcher, J. Henk, A. N. Yaresko, W. Hergert, I. I. Mazin, I. Mertig, and A. Ernst, Phys. Rev. B **86**, 064441 (2012).

[16] P. K. de Boer and R. A. de Groot, Phys. Rev. B **59**, 9894 (1999).

[17] S. Ryee and M. J. Han, Sci. Rep. **7**, 4635 (2017).

[18] Q. Han, H. T. Dang, and A. J. Millis, Phys. Rev. B **93**, 155103 (2016).

[19] J. E. Ortmann, J. Y. Liu, J. Hu, M. Zhu, J. Peng, M. Matsuda, X. Ke, and Z. Q. Mao, Sci. Rep. **3**, 2950 (2013).

[20] T. Ohnishi and K. Takada, Appl. Phys. Express **4**, 025501 (2011).

[21] C. Autieri, M. Cuoco, and C. Noce, Phys. Rev. B **89**, 075102 (2014).